CONFERENCE PRE-PRINT

RESULTS FROM THE LAST DD AND DT JET CAMPAIGNS IN THE FRAMEWORK OF THE EUROFUSION TOKAMAK EXPLOITATION ACTIVITY

N. VIANELLO on behalf of the EUROfusion Tokamak Exploitation Team
Consorzio RFX (CNR, ENEA, INFN, Università di Padova, Acciaierie Venete SpA)
Istituto per la Scienza e la Tecnologia dei Plasmi, CNR
Padova, Italy
Email: nicola.vianello@igi.cnr.it

Abstract

JET, the only tokamak together with TFTR capable of operating with deuterium–tritium (D–T) fuel up to now, has provided critical experimental data to support ITER and DEMO design and operation [1] . Within the EUROfusion Tokamak Exploitation Work Package, JET completed its final campaigns (2022–2023), culminating in the third D–T campaign (DTE3). These experiments addressed key challenges in plasma performance, exhaust control, and tritium management under reactor-relevant conditions. Significant progress was achieved in demonstrating ITER-like integrated scenarios with impurity seeding, achieving partial divertor detachment and high confinement ($H_{98} \approx 0.85$) at 3 MA in D–T plasmas. Advanced regimes such as Quasi-Continuous Exhaust and X-point radiator were successfully achieved in D first, then extend ended to D-T operation, confirming their compatibility with future devices. Studies of peeling-limited pedestals and optimized hybrid scenarios improved understanding, respectively, of edge stability and impurity control in metallic environments. Real-time control systems for D/T ratio regulation and plasma exhaust were deployed, while energetic particle physics investigations revealed turbulence suppression mechanisms linked to fast ions. Operational milestones included a new world record of 69 MJ fusion energy in tritium-rich hybrid plasmas and long-pulse H-mode operation up to 60 s, contributing with unique data to the CICLOP database. Comprehensive tritium retention studies using gas balance, post-mortem analysis, and ITER-relevant laser diagnostics provided essential input for tritium accountancy strategies. These results validate ITER operational concepts, inform DEMO design, and deliver critical experience in nuclear operation and scenario integration.

1. INTRODUCTION

To ensure safe operation margins in next-step fusion devices such as ITER and future power plants, experiments on large tokamaks using deuterium-tritium (D-T) fuel mixtures are essential. These studies provide critical data for understanding plasma physics under conditions approaching those of burning plasmas, while also informing operational procedures and identifying technological challenges.

JET has played a pivotal role in this context for over 40 years [1] , being the only device, together with TFTR, capable of operating with D-T mixtures. Designed as a large tokamak to explore reactor-relevant plasma behaviour, JET was engineered to confine a significant fraction of alpha particles—up to 90% at 2.5 MA.

Following the first D-T campaign (DTE1, 1997) [2] , which revealed unacceptable tritium retention, JET transitioned from carbon to all-metal plasma-facing components (beryllium main chamber, tungsten divertor) [3] , pioneering metallic wall operation in large tokamaks [4] .

In 2021, JET conducted its second D-T campaign (DTE2) [5] , achieving major milestones: a record fusion energy output, improved confinement and reduced energy losses in D-T plasmas compared to pure deuterium, and enhanced understanding of energetic ion dynamics and multiscale transport [5,6]. These results strengthened confidence in predictive modelling and provided new insights into isotope effects, plasma-wall interactions (PWI), and RF heating—key for ITER's D-T operation.

From 2022 to 2023, JET's scientific program was integrated into the EUROfusion Work Package Tokamak Exploitation (WPTE), alongside ASDEX Upgrade, MAST-U, TCV, and WEST. This coordinated effort leveraged the unique capabilities of each device to address key physics questions for ITER and DEMO. This activity culminated with the final JET DT campaigns, DTE3 [7] , and the outcomes of JET's contribution of this campaign as well as the rest of the DD operation in 2022-2023 are presented in this contribution.

2. JET IN WITHIN EUROFUSION TOKAMAK EXPLOITATION WORKPACKAGE

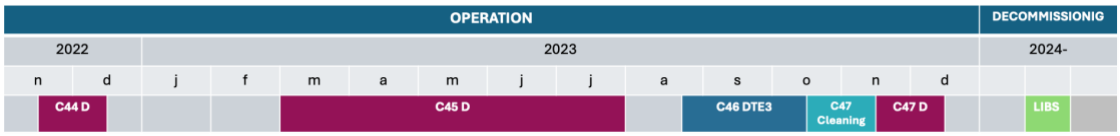

Fig 1: JET timeline for the 2022-2023 period described in the present contribution. Violet indicate operation in Deuterium, Dark Blue operation in DT, Light Blue cleaning operation, Green LIBS operation

Leveraging the capabilities of individual devices, the WPTE program aims to strengthen confidence in scenario extrapolation, key physics understanding, and technical solutions such as control schemes. It adopts a stepladder approach from mid-size tokamaks to JET, enabling exploration of a broader parameter space in terms of size, plasma current, heating mix and power, shaping, and plasma-facing components. JET's contribution has been essential for validating physics models and scenario scalability to larger devices in a metallic environment with higher heating power and isotope mixtures thanks to its T handling capabilities.
The JET experimental program under WPTE spanned about two years (2022–2023) of semi-continuous operation. Fig 1 illustrates the sequence, designed as a single program where D-T operations extended the preceding deuterium campaigns [8]. The program was structured around nine Research Topics [8] , translated for JET into the following priorities:

1. Develop ITER-compatible H-mode scenarios with effective exhaust handling; investigate mechanisms such as peeling-limited pedestal in metallic walls and peripheral high-Z impurity screening and explore them both in single isotope (DD) and mixed isotopes (DT)
2. Explore ELM-free regimes as alternatives to Type-I ELMy scenarios for next-step devices both in DD and in DT
3. Fully exploit Shattered Pellet Injection to inform ITER disruption and runaway electron mitigation strategies.
4. Advance integrated plasma control systems for stable operation and extend them to D-T conditions.
5. Demonstrate the X-point radiator regime for full detachment in DEMO-relevant conditions (D and D-T) and achieve real-time control of divertor detachment in D-T.
6. Expand knowledge of deuterium and tritium retention.
7. Develop stable, steady-state high-β_N operation and control for JT-60SA and DEMO.
8. Investigate fast-ion confinement, turbulence stabilization, and MHD losses to improve burning plasma predictions.

In addition to these pillars, time was allocated to resolve outstanding issues from T and DTE2 campaigns and to address nuclear technology aspects relevant to ITER. All high-level objectives were pursued during DTE3 [7] , except SPI, as its hardware was incompatible with T operation and had to be removed before D-T operations.

DTE3 strongly benefited from DTE2 experience, enabling operational optimizations [9] . Unlike DTE2, both beams in DTE3 were operated in deuterium, offering higher reliability than tritium beams. As before, the campaign was constrained by the JET lifetime limit of 2×10^{21} 14 MeV neutrons. DTE2 and DTE3 together accounted for 86.8% of this budget.

3. PHYSICS AND SCENARIO EXPLORATION TOWARDS ITER AND DEMO

3.1. JET-ITER baseline scenario with Ne seeding

In its 15 MA reference scenario, ITER is expected to operate with a partially detached divertor, achieved through a combination of high divertor neutral pressure and extrinsic impurity seeding [10] , while maintaining high core and pedestal performance. To support this operational point and provide a robust dataset for model validation and scenario extrapolation, JET developed the "*JET ITER baseline*" scenario, designed to reproduce ITER-like plasma shapes and conditions as closely as possible. This effort builds on earlier studies at 2.5 MA/2.7 T in DTE2 [11] , which demonstrated the feasibility of Ne-seeded plasmas with good performance ($H_{98} \approx 0.9$, $\beta_N \approx 2.2$) and high radiation fraction under high-recycling divertor conditions, although the operational domain was limited by the available input power.
Motivated by these promising results, dedicated experiments were conducted in 2022–2023 to expand the operational space and investigate core–edge–exhaust integration in both deuterium and deuterium–tritium plasmas. These discharges were performed at high input power (30–35 MW), with plasma currents of 2.5–3.2 MA,

and in ITER-relevant configurations: high triangularity ($\delta_u = 0.36–0.40$, $\delta_l = 0.35$), $q_{95} = 2.7–3.3$, and a closed divertor geometry with strike points on vertical tungsten tiles (VV configuration, inertially cooled). Partial divertor

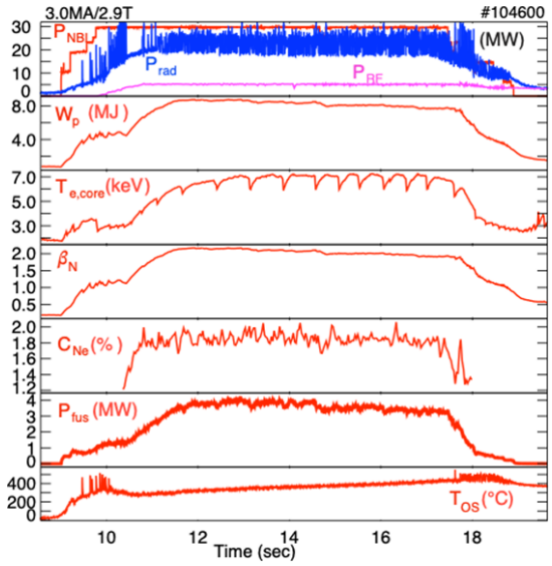

Fig 2: Demonstration of a fully integrated Ne-seeded JET–ITER baseline scenario in D-T at 3 MA/2.9 T, sustained for over 7 s with a partially detached divertor ($P_{in} \approx 34$ MW, $f_{GW} \approx 0.75$, $\beta_N \approx 2$, $H_{98} \approx 0.85$). The discharge achieved ITER-relevant core–edge integration without tungsten accumulation or significant ELM activity, illustrating the feasibility of impurity-seeded operation for heat-flux mitigation while maintaining high confinement

detachment—essential for protecting ITER's divertor from excessive heat flux—was achieved and sustained through neon injection under feedforward control.

At the same time, ITER-relevant pedestal conditions were obtained, with low collisionality ($\nu^{*e,ped} \approx 0.3–0.4$), normalized pressure $\beta_N \approx 2.1$, and small or no ELM activity, without evidence of tungsten accumulation.

Attempts to extend the scenario to 3.2 MA, to further reduce pedestal top collisionality and as well test the scenario to foreseen lower divertor heat flux width λ_q , were technically challenging due to the narrow operational window and the risk of large electromagnetic forces in case of disruption. Even at maximum available power ($P_{in} \approx 37$ MW), plasmas at 3.2 MA/3.45 T could not be sustained in proper H-mode, and only modest performance was achieved at 3.0 MA/2.9 T. In contrast, the Ne-seeded JET–ITER baseline scenario at 2.5 MA/2.7 T in deuterium proved robust, operating close to partial detachment of the outer strike point (OSP) with good confinement ($H_{98} \approx 0.85–1.0$), pedestal temperatures $T_{e,ped} \approx 1$ keV and $T_{i,ped} \approx 1.3–1.9$ keV, pedestal density $n_{e,ped} \approx (4–5)\times10^{19}$ m^{-3} ($\nu^{*e,ped} \approx 0.3–0.7$), and $f_{GW} \approx 0.7–0.8$, with minimal ELM activity. Improved confinement in these conditions resulted from multiple synergistic effects: reduced $n_{e,sep}$ and $n_{e,ped}$, increased $T_{e,ped}$ and $T_{i,ped}$, higher T_i/T_e ratio, enhanced pedestal pressure, and improved core density peaking and rotation [12] .

Operation in D-T further expanded the accessible parameter space, likely due to beneficial isotope effects reducing the L–H power threshold [13] . This enabled the demonstration of a fully integrated Ne-seeded scenario at 3 MA/2.9 T with partial divertor detachment ($P_{in} \approx 34$ MW, $f_{GW} \approx 0.75$, $\beta_N \approx 2$, $H_{98} \approx 0.85$), sustained for more than 7 s without tungsten accumulation or significant ELM activity (Fig 2) [14] . Extensive modelling efforts—combining global gyrokinetic simulations, 2D fluid codes, and integrated reduced models—are ongoing to interpret these improved performances and validate extrapolations to ITER and DEMO.

3.2. W screening experiments

On fusion devices with full tungsten (W) plasma-facing components, high-Z impurity accumulation poses a critical risk due to excessive radiation losses, which can lead to plasma cooling, degraded performance, and even radiative collapse. Among the mechanisms for limiting W accumulation, peripheral screening driven by neoclassical convection is expected to play a key role in ITER [15] , owing to its high pedestal temperature gradient and relatively low density. Neoclassical impurity screening in the plasma edge has been successfully demonstrated in JET hybrid scenarios [16] and confirmed during DTE2 [17] , thanks to the favourable conditions obtained in such scenario, as high input power, low collisionalitty and strong toroidal rotation.

During the DD deuterium campaign in 2022-2023 and subsequent DTE3, further optimization was pursued to further improve W screening studies. Conditions favourable for screening—low pedestal density, high ion pedestal temperature, and strong rotation—were achieved through precise tailoring of gas fuelling timing to ensure

an initially high pedestal temperature, followed by controlled triggering and amplitude of the first ELMs [18] . Additional optimization included reducing plasma current to lower density. When transitioning to D-T in DTE3, the toroidal field was increased to account for the isotope effect on the L–H transition. Examples of achieved edge density and temperature in DD and DT plasmas are shown in Fig 3, in pulses where significant W screening is experimentally observed [19] Confidence on the experimental evaluation of the level of screening, as inferred from bolometry data was improved by optimizing gas injection locations in DTE3 to avoid interference with bolometric reconstruction [17] . Interpretative analysis using the FACIT code [20] is underway to assess whether current modelling capabilities can reproduce the experimentally observed screening levels. Further details are provided in [19,21,22] .

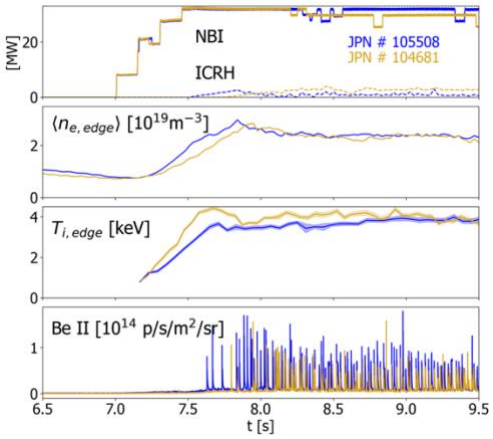

Fig 3: Time traces from a DD (blue) and a DT (gold) hybrid plasma studied for W screening. From top to bottom: NBI and ICRH power, line average density, ion temperature close to pedestal top, Be II line intensity used as ELM monitor. Both the pulses were operated at 2.85T/2.1MA

3.3. Investigation of peeling limited pedestals

Predictive simulations indicate that ITER will operate with a very high pedestal electron temperature ($T_{e,ped} \approx 4$–5 keV) and low collisionality ($\nu^{*ped} \lesssim 0.1$), with the pedestal likely limited by low-n peeling modes [23] . However, these predictions remain uncertain due to their sensitivity to the edge current density near the separatrix. Edge instabilities strongly influence overall plasma performance: in peeling-limited pedestals, pedestal pressure increases with both pedestal and separatrix density, in contrast to ballooning-limited pedestals, where increasing density typically degrades performance.

To date, peeling-limited pedestals have been routinely observed only in carbon-wall devices, with little evidence in metallic environments. Historically, JET-ILW pedestals have been limited by ballooning or coupled peeling–ballooning modes, even at the lowest collisionalities explored, with no clear cases of purely peeling-limited pedestals.

To address this gap and assess the roles of density and isotope mass—critical for ITER predictions—a new operational strategy was implemented on JET. Guided by EUROped simulations, this approach explored high-q_{95} operation (up to $q_{95} \approx 8.5$) by combining low plasma current with high toroidal magnetic field. This configuration stabilizes ballooning modes and enabled unprecedented JET-ILW conditions: $\nu^{*ped} \approx 0.15$ and *normalized radius* $\rho^* \approx 0.002$, much closer to ITER's projected operational space (Fig 4) [24] . The figure illustrates the explored pedestal collisionality range as a function of normalized poloidal radius and separatrix-to-pedestal density ratio, compared with earlier high-δ cases, with indication of the different isotope composition explored.

A density scan in peeling-limited conditions confirmed the predicted positive correlation between pedestal pressure and pedestal density. In contrast, increasing separatrix density had little effect on pedestal pressure, marking a clear difference from ballooning-limited regimes previously observed in JET-ILW. JET's unique capability also enabled an isotope mass scan from pure deuterium to tritium-rich plasmas. Consistent with earlier observations, pedestal pressure increased with isotope mass, primarily due to higher pedestal density rather than changes in pedestal temperature. This suggests that the improvement is not a direct isotope effect on stability but an indirect consequence of density-driven stabilization of peeling modes. More details are given in [25] .

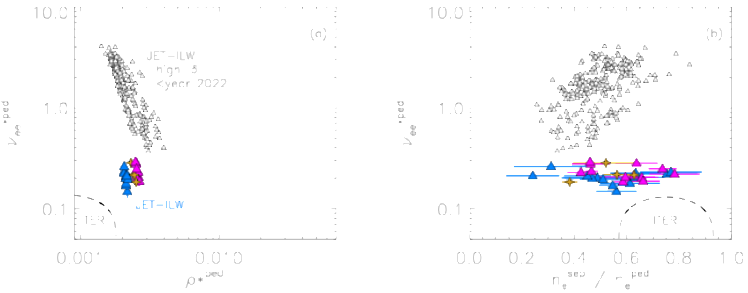

Fig 4: Ranges of pedestal collisionality as a function of normalized poloidal pedestal radius (a) and as a function of separatrix density normalized to pedestal density as explored. In color the explored parameter space with respect to earlier high-delta cases. Colors in the new dataset indicate different isotope compositions: Deuterium (blue points), D-T (gold) and T-rich (magenta)

3.4. No ELM operational scenarios

While ITER plans to operate with RMP-mitigated ELMy scenarios, DEMO-class devices will require robust small-ELM or no-ELM regimes to avoid unacceptable transient heat loads from ELM filaments. Several alternatives were explored during JET's DD operation, including EDA H-mode and negative triangularity, but most experimental time focused on the Quasi-Continuous Exhaust (QCE) scenario. QCE, naturally free of Type-I ELMs, combines high core and edge density with H-mode-grade confinement. Large ELMs are replaced by high-frequency, low-amplitude filaments that spread divertor heat flux to acceptable levels [26] .
Building on experience from medium-size tokamaks [26,27] , the operational window for QCE on JET was established. Key requirements include strong plasma shaping—quantified by the shaping parameter $S_d = \kappa^{2.2}(1+\delta)^{0.9}$ [28] —and high separatrix density. Strong shaping stabilizes global modes, while high separatrix density destabilizes local ballooning modes, triggering benign transport before global instabilities develop. This understanding enabled the determination of an operational point for QCE establishment on JET which nevertheless required careful operation, to cope with additional heat load on upper dump plate which was not designed to handle high heat flux. The operation was successful with the establishment of QCE on JET up to 2.2 MA of plasma current, value so far unexplored in mid-size tokamaks. As a proof of predicting capabilities, Fig 5 illustrates the sensitivity to S_d, comparing Type-I ELMy and QCE regimes in terms of shaping and divertor target temperature.

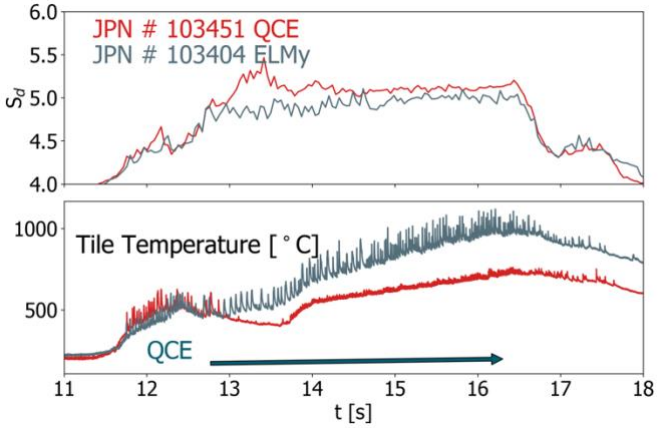

Fig 5: Comparison between JPN 103451 (QCE) and JPN 103404 (ELMy regimes) in terms of shaping parameter and divertor maximum target temperature. Both the shots were operated at 2.8T/2.0MA

JET size allowed access to lower pedestal collisionality than previously achieved [29] , clarifying the roles of separatrix and pedestal-top collisionality in QCE formation. Furthermore, JET's tritium capability enabled the first isotope studies of QCE, confirming its compatibility with D-T plasmas [30] without any major showstopper identified on QCE as a viable reactor scenario candidate. Consistent with DTE2 observations in ELMy regimes, electron pedestal pressure increased when moving from DD to DT, driven by simultaneous rises in density and temperature; ion temperature also increased with isotope mass. No attempt was made to optimize fusion

performance in DT mixtures—the focus was on scenario robustness. Notably, the transition from DD to DT was achieved on the first attempt without significant modification of operational parameters.

3.5. X-Point Radiator Regime

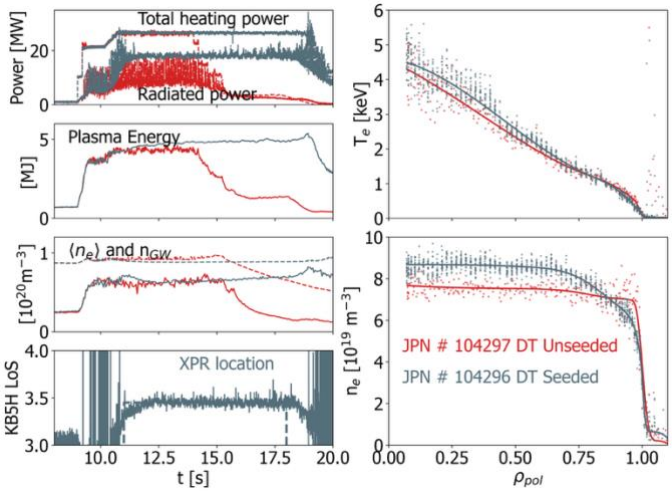

Fig 6: Comparison of seeded and XPR scenarios in DT plasmas. On the left from top to bottom: total heating power and radiated power, Plasma stored energy, core electron density (solid) and corresponding Greenwald density (dashed), Real time detection of XPR. On the right: top panel Temperature profiles, bottom panel Density profiles. Both the shots were operated at 2.65T/2.5MA

Protecting divertor plasma-facing components from extreme heat and particle flux is critical for reactor operation, where DEMO-class devices are expected to operate at high radiation fractions ($f_{rad} \approx 95\%$), exceeding ITER's target. Detached plasma scenarios, which reduce thermal and particle loads on the divertor, are essential to achieve this goal. In 2023, JET conducted extensive detachment studies in deuterium plasmas, later extended to D-T mixtures. Impurity seeding with different species (N, Ne, Ar) was employed to enhance radiative power and facilitate detachment.

Experiments revealed that strong outer divertor detachment is correlated with a localized region near or slightly above the X-point, characterized by intense radiation, low electron temperature (1–2 eV), and high plasma density. This regime, known as the X-point radiator (XPR), has been reproducibly achieved on ASDEX Upgrade, JET, and other devices [31]. XPR scenarios exhibit operational stability, enable full divertor detachment across various impurity seeding mixes, and can suppress ELMs. Crucially, the XPR vertical position can be actively controlled in real time, providing a powerful actuator for detachment regulation [31] .

During JET's 2023 deuterium campaign, XPR scenarios were developed at 2.5 MA/2.65 T, with $P_{in} \approx 25$–27 MW and low-triangularity shapes. The real-time XPR control methodology from ASDEX Upgrade was successfully implemented on JET [32,33] , demonstrating cross-device transferability and compatibility with ITER-relevant diagnostics. For heating powers up to 33MW, a seeding mixture of argon and neon showed the best performance while maintaining DT applicability (where nitrogen is not allowed) avoiding dithering L-H observed in case of pure Ne seeding in this plasma. These plasmas maintained stable H-mode with minimal or no ELM activity and smooth L–H transitions, achieving $H_{98}(y,2) \approx 0.7$–0.8 (vs. ≈ 0.65 unseeded) [31] . Confinement optimization was not a focus of this experiment, and a fusion power of approximately 1.5 MW was produced in DT.

The XPR regime was also demonstrated in stationary D-T plasmas using the same Ar–Ne mixture, confirming robustness and scalability. Noteworthy the real-time control of the XPR position worked smoothly when transferred from DD to DT plasma, exhibiting the same detachment dynamics and proving easy transferability between different isotope mixtures. FigureFig 6 compares seeded and unseeded D-T pulses: seeded cases achieved $f_{rad} > 70\%$, modestly increased stored energy and confinement, and showed no significant pedestal degradation. Kinetic profiles indicate that the energy gain is mainly due to higher plasma density, with minor T_e contribution. Additional DD experiments tested XPR robustness against transients (power steps, pellets), confirming controllability with diagnostics and actuators compatible with nuclear environments.

3.6. Plasma control experiments in JET Deuterium-Tritium Plasmas

In the DTE2 and DTE3 campaigns, a series of advanced real-time controllers—likely to be essential in future nuclear fusion reactors—were successfully deployed. These controllers addressed several operational challenges, including transitions into and out of burn phases, entry into and exit from H-mode, control of plasma exhaust during H-mode, and identification of under-performing plasma discharges (duds) [34,35]
One promising approach for managing burning conditions is controlling the Deuterium/Tritium (D/T) fuel ratio in the reactor. Demonstrating active D/T ratio control in the plasma core is therefore of significant importance.
Figure Fig 7 illustrates this concept. The left panel shows the plasma cross-section of a 1.4 MA / 1.7 T JET pulse (#104651) at 7.4 s. NBI injectors (1–6) used in the experiment are marked in red, while the VHFS pellet injection line is shown in black. The line of sight (LOS) of the HRS (High Resolution Spectroscopy) diagnostic, which provides data for the D/T ratio, is indicated in cyan. Gas injection modules are located at the low-field side (LFS) midplane, approximately marked by a blue rectangle.

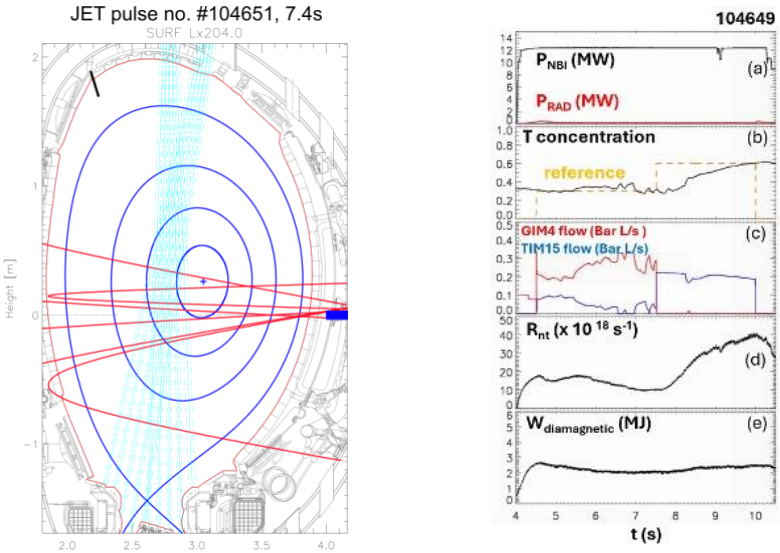

Fig 7: Left panel) Plasma cross-section of 1.4MA/1.7T JET pulse #104651 at 7.4s. NBI injectors 1 to 6 used in this experiment are shown in red, while the pellet VHFS injection line is indicated in black. The LOS of HRS diagnostic providing the data for D/T ratio is shown in cyan. Gas injection modules used in this study are located at the LFS midplane, approximate location is shown by a blue rectangle. (Right panel) Time traces of investigated 1.4MA/1.7T JET pulse #104649 in which D/T ratio was varied by means of D/T gas injection

The right panel of Fig 7 presents time traces from pulse #104649, where the D/T ratio was actively varied using gas injection. Tritium was injected via dedicated gas valves, while Deuterium was introduced through both gas and pellet injection. The D/T ratio was calculated using visible spectroscopy lines of D and T measured in the outer divertor LOS. A real-time algorithm simultaneously controlled the isotope ratio and the total gas injection rate to avoid perturbing other plasma parameters. Each pulse consisted of two distinct phases:

- Phase 1 (4.5–7.5 s): Deuterium-rich plasma was achieved through real-time control.
- Phase 2 (7.5–10 s): The controller adjusted the D/T ratio to a more favourable mix (D/T = 0.4/0.6).

The observed response in DT neutron rate, under constant power and plasma conditions, demonstrates the effectiveness of the controller [36] .
Several discharges were conducted to test the system, using Tritium gas injection and both gas and pellet injection for Deuterium. These experiments were successfully simulated using the TRANSP and JETTO codes [37]. In the simulations, sources from NBI, pellet injection, and gas puffing were treated self-consistently. Particle transport was modelled using a simplified Bohm-gyroBohm approach. JETTO was run predictively for D and T densities, with electron and ion temperatures prescribed from measurements. Particle sources were modelled using FRANTIC (gas injection and recycling), HPI2/continuous pellets (pellet source), and PENCIL (NBI ion source). Impurities and effective charge (Z_{eff}) were modelled using the SANCO code, including Be, Ni, and W. From the physical interpretation, the experiment confirmed that fusion power strongly responds to T injection and concentration, confirming that T fraction is changing as programmed thanks to fast isotope mixing. Furthermore, being the controller based on divertor measurements, this confirm that fraction estimated from divertor region can be considered as representative of core fraction.

3.7. Energetic particle studies

Significant progress was achieved at JET in developing and applying fast-ion diagnostics, including neutron and gamma-ray measurements, to advance understanding of energetic particle (EP) physics [38–40]. Techniques for generating alpha particles in D–^{3}He plasmas were refined by accelerating deuterium NBI ions to higher energies using ICRF, enabling studies of fast-ion-driven instabilities. This approach, relevant for JT-60SA [41,42] —where negative-ion NBI will deliver deuterons at $E_D \approx 500$ keV—also supports the development of alpha-particle diagnostics for ITER [43]. Fast-ion tomography methods were further advanced for analysing past JET D–^{3}He experiments [44]
Progress was also made in understanding fast-ion effects on core turbulence. In JET D-T plasmas with dominant electron heating and ICRF-driven fast ions, improved confinement was observed [45] . Hydrogen minority heating at $n(H)/n_e \approx 1$–1.5% reduced thermal ion heat conductivity in the core, consistent with local gyrokinetic simulations. Global GENE modelling indicated multiple turbulence-suppression mechanisms at different radii [46]. Turbulence reduction was stronger in D-T than in D-D plasmas, possibly linked to enhanced shear flows, as suggested by nonlinear FAR3d simulations [47]. Ongoing analysis aims to exploit these effects for ITER and future devices [48].
Similar turbulence reduction was observed in H-D plasmas using the three-ion ICRF D-(^{3}He)-H scheme, which accelerates ^{3}He ions to MeV energies, producing dominant electron heating and fast-ion-driven AEs [49] . This scenario is relevant for ITER's SRO phase, enabling early validation of EP modelling and diagnostics. ICRF antenna phasing was also explored as an actuator for AE control [41].
Finally, novel ICRF techniques were developed to increase bulk ion temperature using ^{9}Be and argon impurities [41]. Consistent with theory, H minority heating yielded the highest electron temperature, while the three-ion scheme with core impurity resonance [50] produced the highest ion temperature.

3.8. DTE2 Main scenarios

Although with limited machine time attributed, the main scenarios developed in DTE2 were further studied as well in the last JET campaigns.
The ITER-like baseline scenario could not be sustained for long durations in DTE2, although stable operation for ~5 s was achieved in deuterium plasmas [5]. In DTE3, the scenario was revisited to understand why it could not be maintained at the target plasma current of 3.5 MA. Operation at high current above 3.5 MA were nevertheless avoided, as they were posing severe machine risk which could potentially lead to compromised plasma-facing components samples scheduled for post-mortem analysis. At 3.0 MA/2.9 T, MHD activity limited performance when maximum available power was applied. This was mitigated by slightly reducing input power ($P_{NBI} \approx 27$ MW, $P_{RF} \approx 3$ MW), enabling—for the first time—a JET baseline pulse in D-T sustained for 5 s (pulse #104663) until programmed termination, albeit with a slight neutron rate reduction [51]. No further optimization was possible due to time constraints. Current analysis focuses on understanding the challenges of achieving stationary baseline plasmas at high current. However, because of the gas required to maintain the compound ELM activity necessary for the stationarity of the pulse and the lack of optimization, the achieved fusion power was far from the record levels obtained in the hybrid and optimised fuel mix scenarios.
Tritium-rich hybrid pulses in DTE2 delivered a fusion energy record of 59 MJ [52], achieved by optimizing plasma composition and heating. Deuterium NBI heated a tritium-rich plasma to maximize non-thermal fusion reactions, while RF heating at the fundamental D resonance (n = 1) further boosted D-T fusion power [53] by accelerating deuterons. The scenario relied on fast isotope mixing to maintain the D-T ratio [52].
In DTE3, this scenario was revisited to improve stationarity. Increasing P_{RF} from ~3.8 MW to ~5.5 MW enhanced resilience to high-Z impurity accumulation and confirmed reproducibility. As a result, a new world fusion energy record of 69 MJ was achieved.

3.9. Long pulse operation at JET

During the final JET-ILW campaign, long-duration deuterium discharges were performed to assess plasma sustainment over multiple resistive times and study plasma–wall interactions in a full-metal environment [54]. These experiments required major technical adjustments across subsystems, including plasma shape control, machine protection, and diagnostics [55]. They achieved the highest injected energy at JET ($E_{IN} = 450$ MJ), pushing the limits of the inertially cooled divertor and auxiliary heating systems. The results contributed to the multi-machine CICLOP database [56] and supported ITER-relevant developments such as water activation diagnostics [57].

Fig 8: JET-ILW 60s H-mode discharge #105750 (B_0=1.9T, I_P=1.4MA): (a) NBI and ICRH power; (c) Bulk radiated power

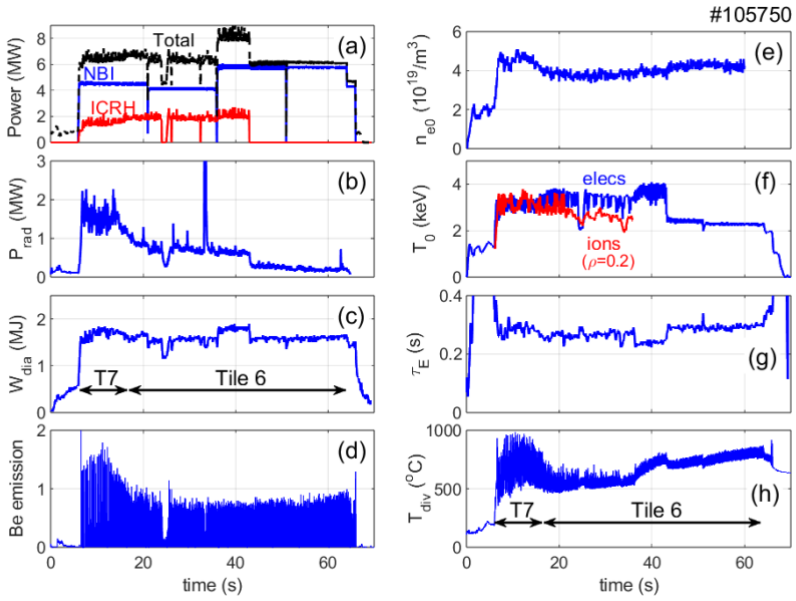

(bolometer); (c) Plasma stored energy; (d) Be-I emission; (e) Central electron density (HRTS); (f) Core electron (ECE) and ion (CXRS) temperatures (g) Energy confinement time (h) Maximum divertor temperature

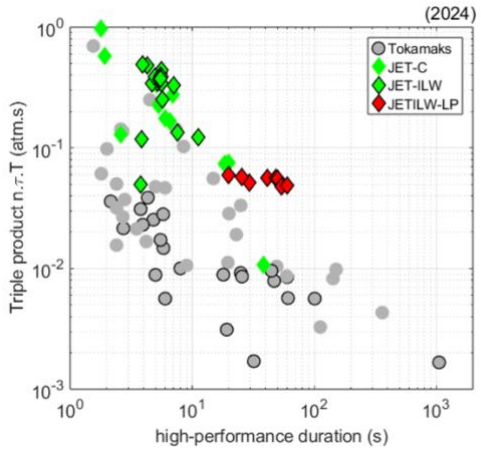

Fig 9: Averaged triple fusion product $n_i.\tau_E.T_i$ as function of the high-performance discharge duration for different tokamaks in the 2024 CICLOP database [56]

Figure Fig 8 shows time traces of a 60 s H-mode discharge (#105750, $B_0 = 1.9$ T, $I_P = 1.4$ MA) with 4–6 MW NBI and 2 MW ICRH for the first 36 s. The strike point was shifted from Tile 7 to Tile 6 to respect divertor energy limits; the Tile 6 phase delivered $E_{IN} = 323$ MJ, slightly above the standard limit (315 MJ), requiring special authorization. Stored energy remained ~1.6–1.8 MJ with $T_{e0} \approx T_{i0} \approx 3.0$–$3.5$ keV during combined heating. After ICRH termination, T_e dropped but W_{dia} stayed constant due to higher density and lower radiation. Energy confinement was steady ($\tau_E \approx 0.25$–0.3 s). Bulk radiation was low during Tile 6, with no impurity accumulation despite a transient event at t = 34 s. Type-I ELMs (50–70 Hz) persisted throughout. Earlier Tile 7 operation showed higher radiation and marginal impurity control due to intermittent ELMs near the L–H threshold. Pulse #105750 consumed ~80% of the available ohmic flux and could have been extended by ~25 s with sustained auxiliary heating [55]. No physics limits were encountered; duration was constrained by engineering factors, mainly auxiliary power and divertor heat handling.

JET-ILW long pulses provided unique data to the CICLOP database, which benchmarks long-pulse performance for future reactors. Figure Fig 9 plots the triple product $n_i \cdot \tau E \cdot Ti$ versus high-performance duration for multiple devices. JET-ILW points (red diamonds) stand out, maintaining $n_i \cdot \tau_E \cdot T_i \approx 0.05$–$0.06$ atm·s with minimal degradation up to 60 s—about five times higher than comparable-duration entries in the 2024 CICLOP dataset. Since these results (Dec 2023), other devices have extended their records; updates will be presented in this conference [58].

3.10. Characterization of fuel retention in JET DT operation

In next-step fusion devices, in-vessel tritium inventory must be strictly limited for safety and optimized for fuel cycle efficiency. Fuel retention in plasma-facing components (PFCs) can be assessed using complementary techniques:

i. **Gas balance** between injected and pumped gas, providing global retention estimates per pulse or per day [59]
ii. **Post-mortem analysis** retrieved samples, yielding campaign-integrated ex situ local measurements and giving insight on retention mechanisms at play [60]
iii. **Laser-based diagnostics**, enabling local in situ measurements, either during campaigns or vent-phase [61]

JET demonstrated a ~10 times reduction in fuel retention when transitioning from carbon to Be-W walls [62]. In deuterium operation, gas balance indicated short-term retention of ~2% of injected fuel, while post-mortem analysis showed ~0.2% retained long-term, mainly via codeposition of D with Be with a significant amount of fuel trapped in the upper tiles of the inner divertor [60].

JET uniquely enables retention studies in DT plasmas, including assessing tritium removal efficiency [63]. fuel retention measurements techniques quoted above were applied during DTE2 and DTE3. Gas balance over full-day operations proved challenging due to low retention levels and tritium-handling complexity, but results indicate comparable fuel retention in D and DT plasmas. Faster post pulse T outgassing compared to D suggests that both the concentration and depth profile of the isotope in the vessel walls might play a role [60]. The global T accountancy based on the Active Gas Handling System (AGHS) of JET is still ongoing for DTE2 and DTE3 and is expected to be completed in 2026. Sample retrieval for postmortem analysis was completed in summer 2025; analysis is ongoing. Those long lead endeavours are key to complement results already obtained from gas balance.

Extensive in situ surface analysis using both laser based diagnostic techniques contemplated for assessing fuel retention in ITER has been performed during DTE3, the subsequent cleaning campaign and following D operation. The Laser Induced Desorption with gas detection using Quadrupole Mass Spectrometers (LID-QMS) was used to monitor weekly retention evolution during DTE3 and cleaning phases [64]. This demonstrated the capability of LID-QMS to discriminate D and T and to quantify the effect of cleaning procedures, such as operating D plasmas in the Raised Inner Strike Point (RISP) configuration to heat the inner divertor tiles prone to codeposition of fuel with Be [60,63].

Laser Induced Breakdown Spectroscopy (LIBS) deployed on JET's robotic arm, was applied for the first time in a DT environment post-vent (fall 2024) [65]. Although T detection was challenging due to low residual T levels after cleaning campaigns and to D and T spectral lines overlap, preliminary results show Be deposition patterns consistent with previous observation and correlation between fuel content (D/H/T) and Be-rich regions.

The lessons learned during JET DT fuel retention experiments, detailed in [59], will be used to inform the strategy for T accountancy in ITER, and the design of the associated diagnostics and operational procedures. The extensive use of LID-QMS and LIBS, combined with the effort required for quantitative interpretation, provides critical operational experience for ITER. More details on the status of fuel retention studies can be found in [66].

4. CONCLUSIONS

The final JET campaigns, conducted within the EUROfusion Tokamak Exploitation framework, have delivered a comprehensive set of results that significantly strengthen the scientific and technological basis for ITER and DEMO. These campaigns demonstrated ITER-relevant integrated scenarios with impurity seeding, achieving partial divertor detachment and high confinement in D–T plasmas, while validating advanced exhaust solutions such as the X-point radiator and Quasi-Continuous Exhaust regimes under reactor-relevant conditions. Extensive studies of pedestal stability, including the first observation of peeling-limited pedestals in a metallic environment at ITER-like collisionalities, provide critical benchmarks for predictive models. Investigations of isotope effects, impurity screening in hybrid scenarios, and turbulence suppression by fast ions have deepened understanding of core–edge integration and transport physics.

Operational milestones included the achievement of a new world record of 69 MJ fusion energy in tritium-rich hybrid plasmas, long-pulse H-mode operation sustained for 60 s, and the deployment of advanced real-time control

systems for isotope ratio regulation and plasma exhaust management. These achievements were complemented by comprehensive tritium retention studies using gas balance, post-mortem analysis, and ITER-relevant laser diagnostics (LID-QMS and LIBS), providing essential input for tritium accountancy and fuel cycle strategies. Collectively, these results validate ITER operational concepts, inform DEMO design choices, and deliver critical experience in nuclear operation, scenario optimization, and integrated control. JET's legacy, still under active data analysis and modelling activities, now provides a robust experimental foundation for the next generation of fusion devices, bridging the gap between present-day tokamaks and burning plasma reactors.

ACKNOWLEDGEMENTS

This work has been carried out within the framework of the EUROfusion Consortium, funded by the European Union via the Euratom Research and Training Programme (Grant Agreement No 101052200 — EUROfusion). The Swiss contribution to this work has been funded by the Swiss State Secretariat for Education, Research and Innovation (SERI). Views and opinions expressed are however those of the author(s) only and do not necessarily reflect those of the European Union, the European Commission or SERI. Neither the European Union nor the European Commission nor SERI can be held responsible for them.

REFERENCES

1. RIMINI, F. G., *et al. Plasma Phys. Control. Fusion* **67,** 033001 (2025).
2. JACQUINOT, J. *et al. Nucl. Fusion* **39,** 235–253 (1999).
3. MATTHEWS, G. F. *et al. Phys. Scr.* **T145,** 014001 (2011).
4. JOFFRIN, E. *et al. Nucl. Fusion* **59,** 112021 (2019).
5. MAGGI, C. F. *et al. Nucl. Fusion* **64,** 112012 (2024).
6. GARCIA, J. *et al. Rev. Mod. Plasma Phys.* **9,** 10 (2025).
7. KAPPATOU, A. *et al. Plasma Phys. Control. Fusion* **67,** 045039 (2025).
8. JOFFRIN, E. *et al. Nucl. Fusion* **64,** 112019 (2024).
9. KING, D *et al. Nucl. Fusion* **64,** 106014 (2024).
10. PITTS, R. A. *et al. Nucl Mater Energy* **20,** 100696 (2019).
11. GIROUD, C. *et al. Nucl. Fusion* **64,** 106062 (2024).
12. MARIN, M. *et al. Nucl. Fusion* **63,** 016019 (2023).
13. SOLANO, E. R. *et al. Nucl. Fusion* **63,** 112011 (2023).
14. CARINE, G. *et al.* this conference
15. DUX, R. *et al. Nucl. Mater. Energy* **12,** 28–35 (2017).
16. FIELD, A. R. *et al. Nucl Fusion* **63,** 016028 (2023).
17. HOBIRK, J. *et al. Nucl. Fusion* **63,** 112001 (2023).
18. KING, D., *et al.* this conference
19. FIELD, A. R. *et al. submitted to Plasma Physics and Controlled Fusion* (2025).
20. FAJARDO, D. *et al. Plasma Phys Contr F* **65,** 035021 (2023).
21. KING, D. B. *et al. submitted to Plasma physics and Controlled Fusion* (2025).
22. KING, D., *et al.* this conference
23. SAARELMA, S. *et al. Nucl. Fusion* **52,** 103020 (2012).
24. FRASSINETTI, L. *et al. Nucl. Fusion* **65,** 076028 (2025).
25. FRASSINETTI, L., *et al* this conference
26. FAITSCH, M. *et al. Nucl. Mater. Energy* **26,** 100890 (2021).
27. LABIT, B. *et al. Nucl Fusion* **59,** 086020 (2019).
28. DUNNE, M., *et al Nucl. Fusion* **64,** 124003 (2024).
29. FAITSCH, M. *et al. Nucl. Mater. Energy* **42,** 101904 (2025).
30. FAITSCH, M. *et al. Nucl. Fusion* **65,** 024003 (2025).
31. BERNERT, M. *et al. Nucl. Mater. Energy* **43** 101916 (2025)
32. BOSMAN, T. O. S. J. *et al. Nucl. Fusion* **65,** 016057 (2025).
33. SIEGLIN, B. *et al. Fusion Eng. Des.* **215,** 114961 (2025).
34. BARUZZO, M., *et al.* this conference
35. PIRON, L., *et al.* this conference
36. Lennholm, M. *et al. PRX Energy* **4,** 023007 (2025).
37. KIROV, K. K. *et al. Nucl. Fusion* **65,** 106016 (2025).

38. KIPTILY, V. G. *et al. Nucl. Fusion* **64,** 086059 (2024).
39. MOLIN, A. D. *et al. Phys. Rev. Lett.* **133,** 055102 (2024).
40. SHARAPOV, S. *et al.,* this conference
41. KAZAKOV, Y., *et al.,* this conference
42. COELHO, R., *et al.,* this conference
43. KIPTILY, V. *et al., Fusion Eng. Des.* **215,** 114959 (2025).
44. REMAN, B. C. G. *et al. Nucl. Fusion* **65,** 076007 (2025).
45. GARCIA, J. *et al. Nat. Commun.* **15,** 7846 (2024).
46. SIENA, A. D. *et al. Nucl. Fusion* **65,** 086019 (2025).
47. VARELA, J. *et al. Nucl. Fusion* **65,** 076044 (2025).
48. MAZZI, S., *et al.*, this conference
49. RUIZ, J. R. *et al. Phys. Rev. Lett.* **134,** 095103 (2025).
50. KAZAKOV, Ye. O. *et al. Phys. Plasmas* **22,** 082511 (2015).
51. GARZOTTI, L., *et al.* EPS 2025 and to be submitted to *Plasma Physics and controlled fusion* (2025).
52. MASLOV, M. *et al. Nucl. Fusion* **63,** 112002 (2023).
53. Lerche, E. *et al.* this conference
54. Lerche, E. A. *et al. Plasma Phys. Control. Fusion* (2025). doi:10.1088/1361-6587/ae006f
55. KING, D. B. *et al. Plasma Phys. Control. Fusion* **67,** 085011 (2025).
56. LITAUDON, X. *et al. Nucl. Fusion* **64,** 015001 (2024).
57. VILLARI, R. *et al. Fusion Eng. Des.* **217,** 115133 (2025).
58. LITAUDON, X., *et al.* this conference
59. LOARER, T. *et al. Nucl. Fusion* **47,** 1112–1120 (2007).
60. WIDDOWSON, A. *et al. Phys. Scr.* **96,** 124075 (2021).
61. PHILIPPS, V. *et al. Nucl. Fusion* **53,** 093002 (2013).
62. BREZINSEK, S. *et al. Nucl. Fusion* **53,** 083023 (2013).
63. MATVEEV, D. *et al. Nucl. Fusion* **63,** 112014 (2023).
64. ZLOBINSKI, M. *et al. Nucl. Fusion* **64,** 086031 (2024).
65. ALMAVIVA, S., *et al.* in *20th International Conference on Plasma-Facing Materials and Components for Fusion Applications* (2025).
66. MATVEEV, D. *et al.* this conference